Nucleic Acids Research, 1997, Vol. 25, No. 20 **4139–4146**

A fiber optic biosensor for fluorimetric detection of triple-helical DNA

André H. Uddin, Paul A. E. Piunno[1], Robert H. E. Hudson[1,+], Masad J. Damha* and Ulrich J. Krull[1,*]

Department of Chemistry, Otto Maas Chemistry Building, McGill University, Montreal, Quebec H3A 2K6, Canada and [1]Chemical Sensors Group, Department of Chemistry, Erindale College, University of Toronto, Mississauga, Ontario L5L 1C6, Canada

Received May 13, 1997; Revised and Accepted August 22, 1997

ABSTRACT

A fiber optic biosensor was used for the fluorimetric detection of T/AT triple-helical DNA formation. The surfaces of two sets of fused silica optical fibers were functionalized with hexaethylene oxide linkers from which decaadenylic acid oligonucleotides were grown in the 3′ to 5′ and 5′ to 3′ direction, respectively, using a DNA synthesizer. Fluorescence studies of hybridization showed unequivocal hybridization between oligomers immobilized on the fibers and complementary oligonucleotides from the solution phase, as detected by fluorescence from intercalated ethidium bromide. The complementary oligonucleotide, dT_{10}, which was expected to Watson–Crick hybridize upon cooling the system below the duplex melting temperature (T_m), provided a fluorescence intensity with a negative temperature coefficient. Upon further cooling, to the point where the pyrimidine motif T*AT triple-helix formation occurred, a fluorescence intensity change with a positive temperature coefficient was observed. The reverse-Hoogsteen T·AT triplex, which is known to form with branched nucleic acids, provided a corresponding decrease in fluorescence intensity with decreasing temperature. Full analytical signal evolution was attainable in minutes.

INTRODUCTION

With recent advances in nanotechnology (1), there is an increased demand to investigate biomolecular structure and behavior (2). One particular area of interest stems from the progress in the synthesis of novel nucleic acid macromolecules. Dendrimers (3,4), circular (5) and cage oligonucleotides (6) have been synthesized and these novel compounds are finding applications in biotechnology (7,8).

Furthermore, there is much interest in the development of devices for rapid diagnostic assays to detect microorganisms, viruses and genetic mutations based on hybridization with immobilized nucleic acid probes. Approaches involving electrochemical (9), acoustic wave or piezoelectric (10), plasmon resonance (11,12), colorimetric sensing of non-particle aggregates (13) and fluorescence based optical fiber sensing techniques have been proposed (14–16). In these examples, identification of the analyte is based on the occurrence of Watson–Crick hybridization events, with the formation of three-stranded structures, or triplexes, being largely ignored.

Triple-helical oligonucleotides have potential use as sequence specific artificial nucleases (17), modulators of DNA-binding proteins/gene expression (18,19; for a recent review see ref. 20), materials for genomic mapping (21), and sensitive screening reagents to detect mutations within duplex DNA (22). Formation of three-stranded helices by nucleic acids is a well-known phenomenon which involves a third strand interacting with a purine rich strand in the underlying Watson–Crick DNA duplex (23,24). Two distinct classes of DNA triple-helices have been characterized which differ in the composition and orientation of the third strand relative to the Hoogsteen binding partner (25–32). Nucleic acid binding ligands can be used to identify DNA structures and morphology. For example, ethidium bromide binds to both duplexes and triplexes by intercalation (33), but there is a marked difference in the binding efficiency and fluorescence quantum efficiency between both types of complexes (34–36).

We have focused on the use of a nucleic acid binding ligand (e.g., ethidium bromide) and fluorescence transduction strategy to investigate oligonucleotide hybridization on fused silica optical fiber surfaces. Previously, we reported detection of hybridization events between fibers derivatized with single-stranded deoxyribonucleic acid and complementary DNA and RNA from solution (14). Herein, we report the use of optical biosensor technology for rapid detection of T/AT triplex formation in both parallel and antiparallel configurations. This rapid and efficient triple-helical assay may be extended to include diagnostic assays for sequence-specific duplex recognition, monitoring *in vivo* concentration of gene therapy pharmaceuticals, and for studying properties of synthetic oligonucleotides.

*To whom correspondence should be addressed. (M.J.D.) Tel: +1 514 398 7552; Fax: +1 514 398 3797; Email: damha@omc.lan.mcgill.ca
(U.J.K.) Tel: +1 905 828 5437; Fax: +1 905 828 5425; E-mail: ukrull@credit.erin.utoronto.ca

+Present address: Department of Chemistry, University of Western Ontario, London, Ontario, Canada

The authors wish it to be known that, in their opinion, the first two authors should be considered as joint First Authors

MATERIALS AND METHODS

Chemicals

Reagent grade solvents were purchased (BDH, Toronto, ON) and further purified or dried by standard laboratory practices. DNA synthesis reagents and decadeoxyadenylate (dA_{10}) were purchased from Dalton Chemical Laboratories Inc. (Toronto, ON) and were used as received or were prepared as below. Anhydrous acetonitrile (Dalton) was predried by distillation from P_2O_5 and redistilled from calcium hydride under dry argon. Tetrahydrofuran (BDH) was predried over CaH_2, filtered and distilled immediately prior to use from sodium metal (Aldrich)/benzophenone (Aldrich). Ethidium bromide (3,8-diamino-5-ethyl-6-phenylphenanthridinium bromide; Aldrich) was used as received. Water was double-distilled in glass, treated with diethyl pyrocarbonate (Aldrich) and autoclaved. Molecular biology grade polyacrylamide gel electrophoresis reagents and apparatus were obtained through Bio-Rad (Hercules, CA). Silica gel (Toronto Research Chemicals, Toronto, ON) had a particle size of 30–70 microns. Pre-cut fused silica optical fiber pieces with a length of 48 mm and a core diameter of 400 µm having both termini polished to within a 0.3 µm tolerance were obtained from 3M Specialty Optical Fiber (North York, Ontario, Canada) in addition to lengths of fiber having the same core material and diameter with a TECS 48 low refractive index outer cladding (0.48 numerical aperture).

Derivatization of optical fibers

Synthesis of DMT-HEG (dimethoxytrityled hexaethylene glycol). A solution of dimethoxytrityl chloride (7.1 g, 21 mmol) in dry pyridine (10 ml) was added dropwise to a stirred solution of hexaethylene glycol (HEG, 5.6 ml, 21 mmol in 5 ml pyridine) under an argon atmosphere. Stirring was continued overnight after which the reaction mixture was combined with dichloromethane (50 ml). The mixture was then shaken with 5% aqueous bicarbonate (2 × 90 ml) and then with water (2 × 90 ml) to remove unreacted HEG, pyridine and salts. The organic layer was dried under reduced pressure to yield the crude product. The product was purified by silica gel column chromatography using an eluent of 1:1 dichloromethane/diethyl ether containing 0.1% triethylamine (2.9g, 24% yield). The identity of the product was confirmed by proton NMR spectroscopy. R_f (silica gel thin-layer chromatography): 0.10 in CH_2Cl_2/ether (1:1). ^1H NMR (200 MHz, $CDCl_3$) δ: 7.48 (t, 1H, J = 1.8 Hz), 7.46–7.42 (m, 2H), 7.27 (d, 1H, J = 2.6), 7.3 (d, 1H, J = 3.3 Hz) , 7.1 (m, 8H), 3.79 (s, 6H), 3.64 (s, 24H).

Surface preparation of optical fibers. The coating material was mechanically stripped from the pre-cut optical fiber pieces and the cladding dissolved by treatment with acetone. The surface of the fibers were then cleaned via treatment with 25% ammonia/30% hydrogen peroxide/water (1:1:5, v/v/v) for 5 min at 80 °C followed by rinsing with 30% hydrogen peroxide. The fibers were then treated with a solution of conc. HCl/30% hydrogen peroxide/water (1:1:5, v/v/v) for 5 min at 80 °C, followed by rinsing with methanol, dichloromethane and diethyl ether.

Functionalization of optical fibers with 3-glycidopropyltrimethoxysilane (GOPS). Following a modification of the method reported by Maskos and Southern (37), optical fibers and silica gel were activated by placement into a solution of xylene/GOPS/diisopropylethylamine (100:30:1 v/v/v). The reaction was permitted to proceed with gentle agitation for 24 h under nitrogen at 80 °C. The fibers and silica gel were rinsed with methanol, dichloromethane and diethyl ether.

Linkage of DMT-HEG to GOPS functionalized optical fibers. The fibers and silica gel were then functionalized with monotritylated hexaethylene glycol (DMT-HEG) (250 mg, 0.46 mmol) in 30 ml of xylene containing a catalytic amount of sodium hydride with gentle agitation at 40 °C. Silica gel samples (~10 mg) were taken from the reaction mixture daily to determine the loading of DMT-HEG, and this was presumed to indicate loading on the activated fibers. The silica gel samples were immediately washed with 10 ml portions of dichloromethane until the wash solution showed no absorption at 504 nm upon treatment with trichloroacetic acid. The GOPS-HEG-DMT functionalized silica gel samples were then dried under reduced pressure and treated with 5 ml of 5% trichloroacetic acid in dichloroethane in order to liberate the dimethoxytrityl moieties from the hexaethylene glycol chains. The absorbance (504 nm) of the resulting solution was then determined to quantitatively measure the loading of immobilized DMT-HEG. This analysis indicated that the reaction had gone to completion after 7 days. After this time, the fibers were removed from the reaction mixture, washed with dichloromethane and dried by storage *in vacuo* and over P_2O_5 overnight.

The secondary hydroxyl groups produced after reaction of the HEG linker with the epoxide moieties and all other silanols were capped via treatment with trimethylsilyl chloride in pyridine (1:10 v/v) under argon at room temperature for 16 h followed by treatment with acetic anhydride/*N*-methylimidazole/collidine in THF to prevent unwanted oligonucleotide growth at these sites (38). The fibers were then washed sequentially with pyridine, dichloromethane, methanol and diethyl ether and stored *in vacuo* and over P_2O_5. The amount (or 'loading') of DMT-HEG spacers on the surface of a fused silica fiber was ~1 nmol/fiber (48 mm in length).

Synthesis of oligonucleotides on optical fibers

Approximately 10 functionalized DMT-HEG-GOPS fibers (48 mm in length) were placed in a standard 10 µmol scale Applied Biosystems synthesis column and capped with acetic anhydride prior to DNA synthesis using the ABI supplied cycle. Detritylation was performed with 3% trichloroacetic acid in dichloroethane. Activation of phosphoramidites was achieved with 0.5 M tetrazole in acetonitrile. Reagents for capping were as follows: Cap A, phenoxyacetyl anhydride Cap A reagent from Millipore (Mississauga, ON); and Cap B, 16% *N*-methylimidazole in THF (w/v). Iodine, 0.1 M, in THF/pyridine/water (25:20:2, v/v/v) was used for oxidations. Phenoxyacetyl protected dG, dC, dA phosphoramidite monomers were obtained from Millipore. N^6-phenoxyacetyl-3′-*O*-DMT-2′-deoxyadenosine-5′-*O*-[(β-cyanoethyl)*N*,*N*-diisopropyl]-phosphoramidite was prepared via standard protocols (39). The oligomers were deprotected with conc. NH_4OH solution for 2 h at room temperature. Following deprotection, the ammonia solution was collected, the column was washed with autoclaved water and the eluent was also kept. Quantitation of the eluents at 260 nm indicated that ~20% of the oligomers remained bound to the fiber surface.

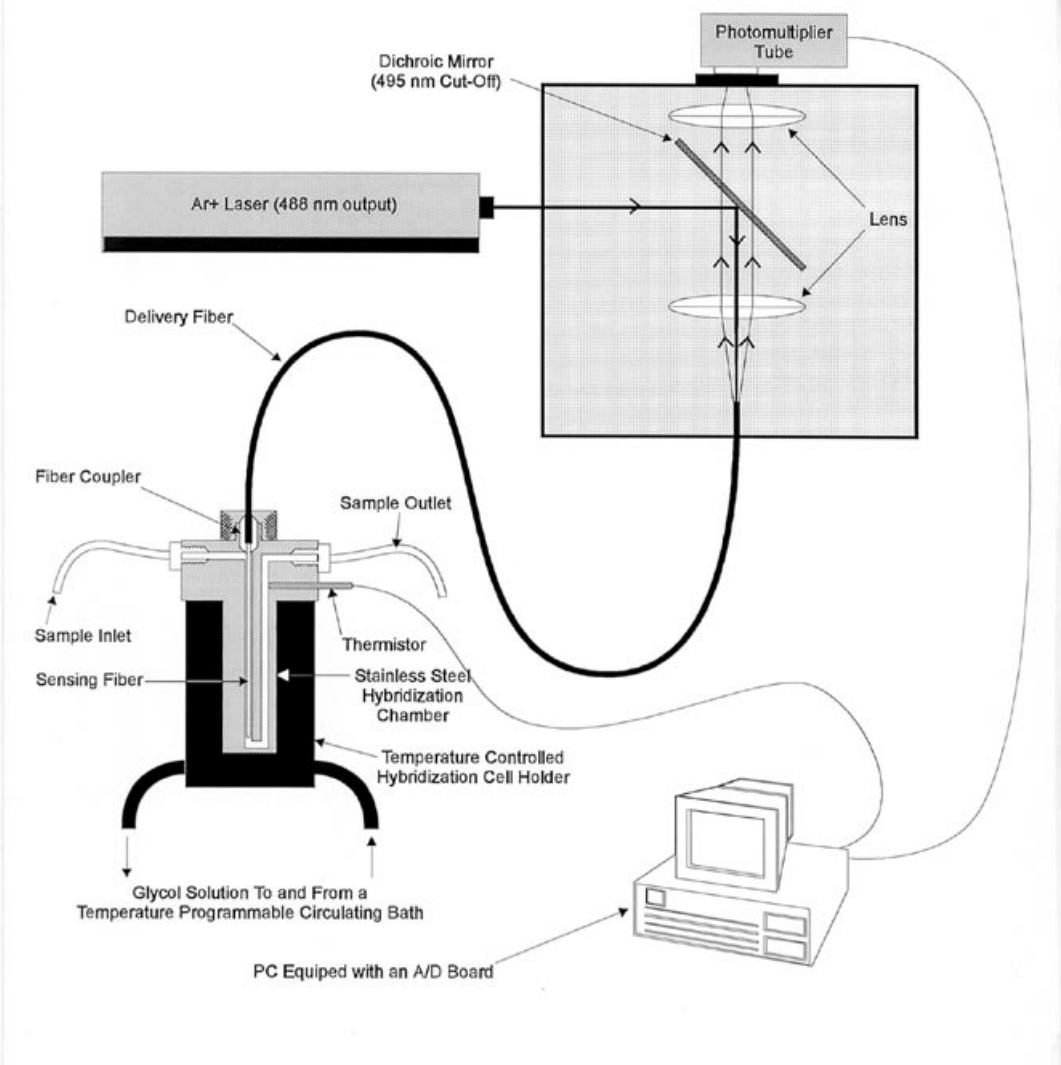

Figure 1. Schematic diagram of the apparatus used for fluorescence investigations of nucleic acid hybridization on the fiber optic sensor.

Synthesis of branched oligonucleotides

The 'V' branched sequence **1** (Fig. 3) was synthesized on an Applied Biosystems 381A instrument using a 1 µmol scale synthesis cycle and β-cyanoethylphosphoramidite chemistry (3,40). Purification, desalting, and analysis of the branched oligonucleotide **1** was accomplished by our detailed protocols (3,41). Typical isolated yields of this branched oligomer were 15–25% (~0.4–1.5 mg), as determined by absorption at 260 nm.

UV thermal denaturation and renaturation studies

Absorbance versus temperature profiles of the nucleic acid complexes (10 mM Tris, 50 mM $MgCl_2$, pH 7.3, 2.5×10^{-8} M ethidium bromide) were measured at 260 nm using a Varian Cary I UV-VIS spectrophotometer. Thermal denaturation profiles (i.e., melting curves) and thermal renaturation profiles (i.e., cooling curves) of each system of oligonucleotides were acquired at two temperature ramp rates, 0.5°C/min and 0.06°C/min. For each system of oligonucleotides, the denaturation and renaturation profiles provided identical results for the melting temperature (T_m) and showed no dependence on the temperature ramp rate used. Normalized plots were constructed according to the method of Kibler-Herzog *et al.* (42). All complexes showed sharp melting transitions. The values of T_m were determined from the first derivative of each thermal curve with an error in precision not greater than ±0.5°C based on variance in repeated experiments.

Instrument setup and fluorescent measurements

The instrument used for fluorescence intensity measurements was based on a fluorescence microscope as was previously described by Krull and co-workers (43) and shown in Figure 1. Radiation from an Ar^+ laser operated at 488 nm was reflected by the dichroic mirror (495 nm cut-off) in the fluorescence microscope to a Zeiss 16× immersion lens with a numerical aperture of 0.5 (Empix Imaging, Mississauga, ON, Canada). The laser radiation exciting the immersion lens was coupled into a delivery fiber of similar numerical aperture (0.48) aligned beneath the objective. The light was totally internally reflected along the length of the delivery fiber to a sensing fiber functionalized with immobilized oligonucleotide. Coupling of the radiation between fibers was achieved by abutting the distal

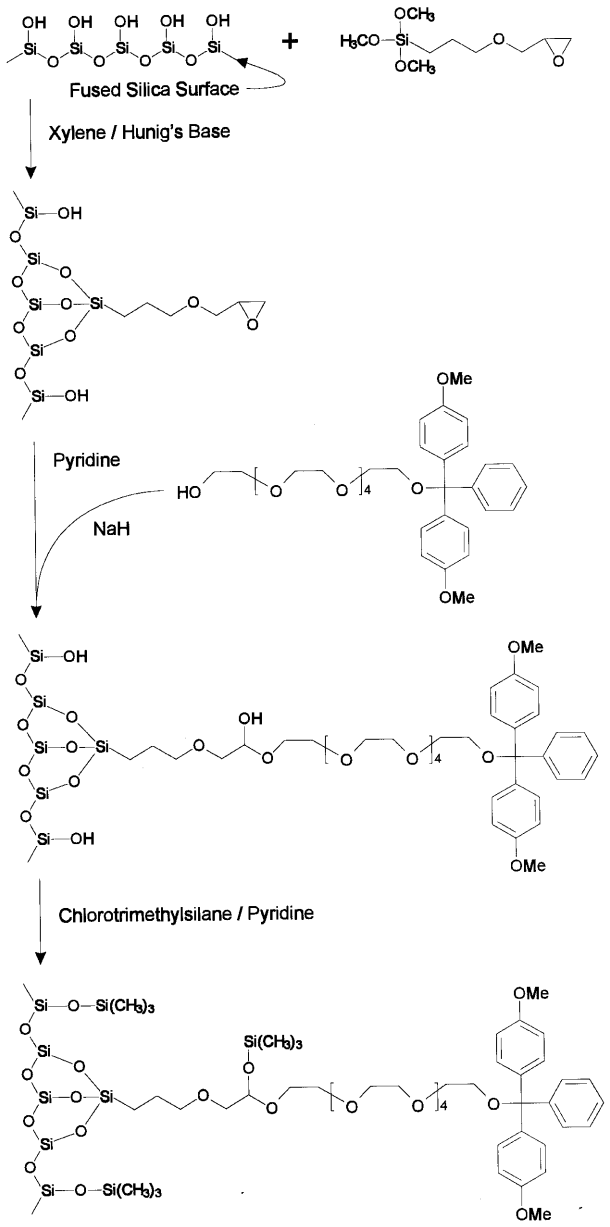

Figure 2. Derivatization of fused silica optical fibers.

terminus of the delivery fiber to the proximal terminus of the sensing fiber. A loss in optical transmission of no more than 2% was observed for the coupled system. The termini of the teflon fiber coupler were designed as compression-fit ends which provided a solution-tight seal that prevented contaminants from diffusing into the fiber coupler and causing drift in the analytical signal. The sensing fiber was placed in a small volume, stop-flow, stainless steel hybridization chamber (1.5 mm i.d. × 48 mm) which provided a solution volume of 79 µl immediately surrounding the sensing fiber. The temperature of the hybridization cell was controlled by placing the cell in a thermostated housing. The temperature of the solutions in the hybridization cell were accurately determined (±0.2°C) by use of a glass encapsulated thermistor incorporated into the hybridization cell. Solutions containing hybridization buffer, ethidium bromide, and complementary nucleic acid sequences were delivered to the

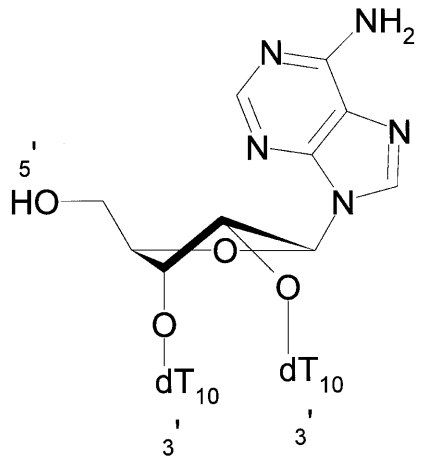

Figure 3. The chemical structure of compound **1**, a branched oligonucleotide with identical chains linked to the 2′- and 3′-positions of a ribose branch-point nucleoside, i.e., rA[(2′-5′-dT_{10})/(3′-5′-dT_{10})]. Ad, adenosine; Th, thymine. Two molecules of dT_{10} hybridize with dA_{10} to give the more common parallel (T*AT, Hoogsteen) triplex, whereas **1** forms a triplex in an antiparallel (T·AT, reversed-Hoogsteen) binding motif.

hybridization cell and sensing fiber by use of a peristaltic pump. In all cases, a hybridization buffer/dye solution of 10 mM Tris, 50 mM $MgCl_2$, 2.5×10^{-8} M ethidium bromide at pH 7.3 was used unless otherwise specified. Fluorescence emission from ethidium bromide that was intercalated into immobilized nucleic acid complexes was totally internally reflected within the sensing fiber and directed towards a photomultiplier tube, where the fluorescence intensity could be quantitatively measured. Drift caused by variations in the efficiency of optical coupling, laser intensity and photomultiplier gain were obviated by normalization of all signals to that of a standard solution of ethidium bromide at 25°C prior to and at the completion of each analysis.

PAGE mobility retardation assay

The solutions of oligonucleotides (10 µl of 30% sucrose/50 mM $MgCl_2$) were incubated at 4°C (96 h) then loaded onto a non-denaturating 15% polyacrylamide gel (90 mM Tris–borate/50 mM $MgCl_2$, pH 8.0). The gels were run at 12.5 mA for 12 h after which the bands in the gel were visualized and photographed by UV illumination followed by ethidium bromide staining.

RESULTS AND DISCUSSION

A goal of this research endeavor was to create a rapid and reliable assay for the detection of triple-helical nucleic acid formation as an extension of work initiated for the detection of duplex formation (14). As a starting point, we chose to investigate the parallel and antiparallel T/AT triplexes as these have been well documented in the literature. Branched nucleic acids as described by Damha *et al.* (3,40) were also used in this study as their unique architecture has been shown to stabilize reversed-Hoogsteen T·AT (antiparallel) triplexes (44). The advantage provided by our optical sensor technology over standard fluorometric work include the low detection limits, reusability and reliability of the device, the non-destructive nature of the assay (where samples may be collected and re-used) and this approach readily lends

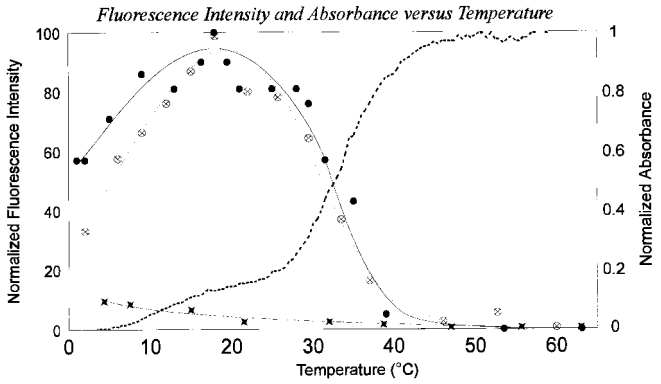

Figure 4. Fluorescent intensity as a function of temperature dA_{10} functionalized sensors challenged with dT_{10}. Response of the optical sensor to 2.5×10^{-8} M ethidium bromide (solid star). Response of the optical sensor with 5′→3′-fiber immobilized dA_{10} to 40 pmol of linear dT_{10} in the presence of 2.5×10^{-8} M ethidium bromide (closed circle). Response of the optical sensor with 3′→5′-fiber immobilized dA_{10} to 40 pmol of linear dT_{10} in the presence of 2.5×10^{-8} M ethidium bromide (cross in open circle). Cooling profile of the same nucleic acid system in bulk solution by measurement of absorbance at 260 nm (thick broken line).

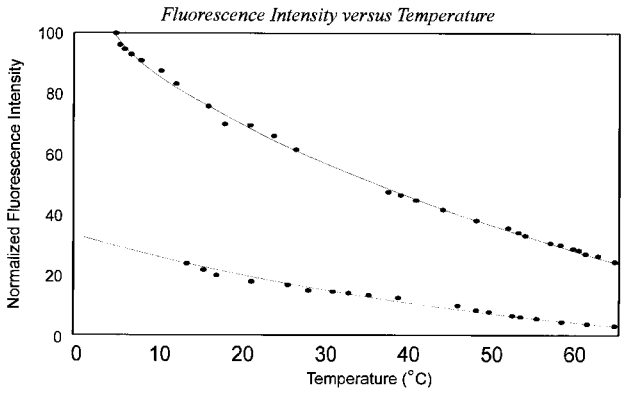

Figure 5. Fluorescent intensity as a function of temperature for the mixed base sequence icosanucleotide functionalized fibers. Upper curve: response of the optical sensor to 20 pmol of linear complement icosanucleotide in the presence of 2.5×10^{-8} M ethidium bromide. Lower curve: response of the optical sensor to 2.5×10^{-8} M ethidium bromide.

itself to automation, thereby negating the requirement of highly skilled technicians to carry out the assay.

Immobilization of oligonucleotides onto optical fibers

The hydroxylated surfaces of the fused silica optical fibers were activated by reaction with GOPS followed by extension with a DMT-HEG linker (Fig. 2). This provides a derivatized surface consisting of a hydrophilic, long-chain spacer arm with a DMT-protected hydroxyl terminus onto which oligonucleotides may be assembled via solid-phase phosphoramidite synthesis (Materials and Methods). This linker was chosen because it is stable to standard oligonucleotide deprotection conditions (37), and provides a fluid environment which facilitates hybridization between immobilized DNA strands and the target strands in solution (47).

Parallel and anti-parallel T-AT triplex considerations

Formation of the intermolecular triplex $2\times dT_{10}:dA_{10}$ may be characterized by a variety of techniques including UV melting studies, molecular modeling, circular dichroism and NMR spectroscopy (48,49). In the pyrimidine motif, the third dT_{10} strand interacts by means of Hoogsteen hydrogen bonds with the dA_{10} strand in target duplex, and is oriented parallel to it. In melting experiments (Mg^{2+} buffer), the triplex $2\times dT_{10}:dA_{10}$ has two resolved transitions, one for dissociation of the third strand from the duplex, i.e., $dT_{10}{*}dA_{10}:dT_{10} \rightarrow dT_{10} + dA_{10}:dT_{10}$ (T_m = 18°C), and one for dissociation of the duplex into its component strands, i.e., $dA_{10}:dT_{10} \rightarrow dA_{10} + dT_{10}$ (T_m = 32°C) (50). Thus association of the third (dT_{10}) strand with the duplex ($dA_{10}:dT_{10}$) is thermodynamically weaker than duplex formation itself (51).

Work done in our laboratories has shown that branched oligonucleotides are useful probes for stabilizing triplex DNA (44). The branched oligomer **1** (Fig. 3) for instance, binds to dA_{10} via reversed-Hoogsteen interactions to give a three-stranded complex in which both dT_{10} strands are antiparallel to the purine (dA_{10}) strand. The formation of this triplex was induced by linkage of two dT_{10} strands through their 5′-ends via coupling to

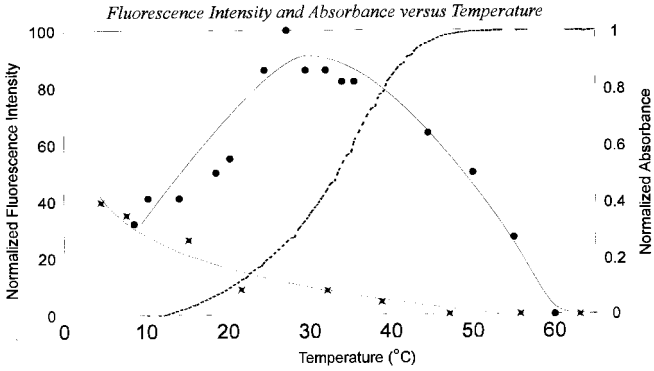

Figure 6. Fluorescent intensity as a function of temperature for **1** using reversed orientation 3′-dA_{10}-5′-fiber derivatized sensors. Response of the optical sensor to 40 pmol of **1** in the presence of 2.5×10^{-8} M ethidium bromide (closed circle) and to the 2.5×10^{-8} M ethidium bromide solution alone (solid star). Cooling profile of the same nucleic acid system in bulk solution by measurement of absorbance at 260 nm (broken line).

riboadenosine at the neighboring 2′ and 3′ oxygen atoms. Although this motif had been observed for T-AT bases in complexes dominated by pur·pur:py bonding (e.g., G·GC, A·AT) (52,53), it has only been observed recently for $dT_n:dA_n$ complexes (44,54). Thermal denaturation and renaturation profiles of a mixture of **1** and dA_{10} (1:1) in Mg^{2+} buffer show a single transition from bound to unbound complex (44), consistent with its formation involving a single bimolecular step, i.e., **1** + $dA_{10} \rightarrow$ triplex **1**:dA_{10} (T_m = 35°C).

Triplex studies using derivatized optical fibers with normal (5′-dA_{10}-3′-fiber) oligonucleotide orientation

Decadeoxyadenylic acid (dA_{10}) was grown in the conventional 3′ to 5′ direction from the fiber surface. Solutions of hybridization buffer containing ethidium bromide, ethidium bromide with dT_{10} or ethidium bromide with **1** were heated (~60°C) in the hybridization chamber containing the decaadenylic acid functionalized optical fibers and renaturation was followed spectroscopically. Fluorescence intensity as a function of temperature for 5′-dA_{10}-3′-fiber functionalized sensors challenged with dT_{10}/ethidium bromide is shown in Figure 4. As

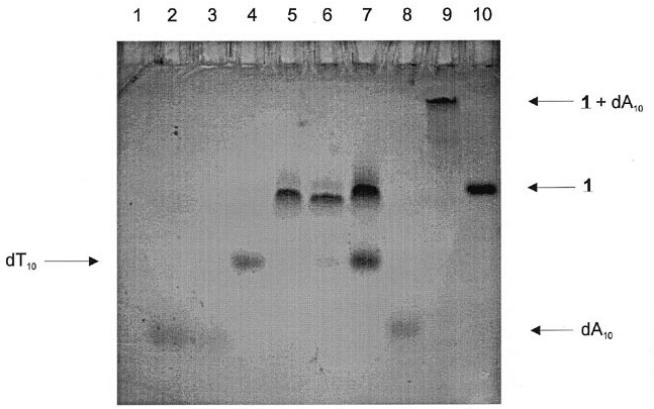

Figure 7. Photograph of a UV-shadowed native polyacrylamide gel containing single strands, duplex and triple helical complexes of branched and linear controls. DNA samples were loaded in 50 mM $MgCl_2$, and 30% sucrose. Lane 4, dT_{10}; lane 5, dT_{10}:dA_{10} (1:1); lane 6, dT_{10}:dA_{10} (2.5:1); lane 7, dT_{10}:dA_{10} (4:1); lane 8, dA_{10}; lane 9, **1** + dA_{10}; lane 10, **1**. As can be noted, the dT_{10}:dA_{10} triplex (lane 7) showed a slight retardation in the mobility relative to the corresponding duplex (lanes 5 and 6). The slowest mobility was observed in lane 9 for the branched triplex **1**:dA_{10}.

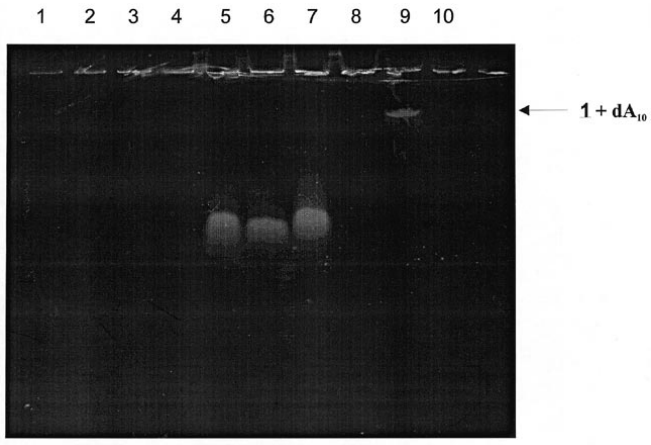

Figure 8. Photograph of an ethidium bromide-stained native polyacrylamide gel (same gel as Fig. 7) containing single strands, duplex and triple helical complexes of branched and linear controls. DNA samples were loaded in 50 mM $MgCl_2$, and 30% sucrose. Lanes 4–10 are the same as those indicated in Figure 7. As can be noted, the dT_{10}:dA_{10} triplex (lane 7) showed a slight retardation in the mobility relative to the corresponding duplex (lanes 5 and 6). The slowest mobility was observed in lane 9 for the branched triplex **1**:dA_{10}. Note that only the duplexes and triplexes showed ethidium bromide fluorescence.

the temperature was lowered to 20°C, there was an increase in the fluorescence intensity due to the quantum yield enhancement of the duplex intercalated ethidium bromide. Upon further cooling, a decrease in the fluorescence intensity with decreasing temperature was observed, indicative of ligand exclusion due to triplex formation (2×dT_{10}:dA_{10}). In order to verify that triplex formation was alone responsible for the exclusion of the ethidium cation and the resulting decrease in fluorescence intensity, a control experiment was done using optical fibers functionalized with a 20 nt sequence of mixed base composition. Because this sequence lacked a pyrimidine $(Py)_n$ or purine $(Pu)_n$ stretch, only a double-stranded complex could form on the surface of the optical sensor upon binding to a complementary sequence. The hybridization experiment was carried out under the same conditions as for the dA_{10} functionalized fibers with the exception of the hybridization buffer (1 M NaCl, 50 mM PO_4^{2-}, pH 7.0). Intense fluorescence with a negative temperature coefficient was observed for the duplex system over the temperature range studied (10–65°C, T_m = 73°C). The control experiment with ethidium bromide and no complementary oligonucleotide showed a negative temperature coefficient over the same temperature range with no such dramatic increase in intensity (Fig. 5).

Interestingly, upon exposure of the optical sensor to the reversed-Hoogsteen forming **1**, no significant increase in fluorescence intensity over that of the ethidium bromide alone in solution was observed (data not shown). The geometrical constraints of compound **1** are such that, if a complex formed with the immobilized dA_{10} strand in this particular (fiber-3′-dA_{10}-5′) orientation, the branch-point riboadenosine moiety would be oriented toward the fiber surface, and thus present a steric barrier to triplex formation. In order to facilitate the formation of the desired antiparallel branched triplex (and test whether steric interference surrounding the branch-point prevented triple-helical formation), an optical sensor having dA_{10} strands in the opposite orientation from the surface, i.e., fiber-5′-dA_{10}-3′, was prepared.

Triplex studies using derivatized optical fibers with reversed (3′-dA_{10}-5′-fiber) oligonucleotide orientation

The fluorescence intensity versus temperature profile with dT_{10} shows an initial increase in fluorescence intensity with decreasing temperature, indicative of duplex formation (Fig. 4). With further cooling of the system, the polarity of the fluorescence intensity temperature coefficient then inverts, indicative of triplex formation. Treatment of the optical sensor with **1** also provided a fluorescence intensity with a positive temperature coefficient at temperatures below the T_m (35°C), indicative of the formation of the reverse-Hoogsteen complex (Fig. 8).

The results of these experiments can be best understood by considering the two key competing factors which influence the net fluorescence intensity temperature coefficient. Firstly, the fluorescence quantum efficiency of the intercalant ligand bound to triple-stranded nucleic acids is greater than that of the ligand bound to double-stranded nucleic acid (36,45,46). This is the result of the triple-stranded structure being more rigid than the double-stranded nucleic acid structure, thereby providing superior shielding of the intercalated fluorophore from non-radiative collisional deactivation. In both cases, triplex and duplex, the quantum efficiency of the bound fluorophore increases with decreasing temperature (i.e., displays a negative temperature coefficient) owing to the overall reduction in the molecular motion in the system. The second factor influencing the net fluorescence emission is the binding efficiency of the intercalant ligand to each substrate type. Not as many ethidium cations can be accommodated per base triplet as per base pair. In addition, further exclusion of ethidium cation occurs with decreasing temperature in triple-helical nucleic acids, thereby providing a fluorescence intensity with a positive temperature coefficient. At low temperatures, the exclusion process dominates the fluorescence signal, thereby providing a means for elucidation of triple-strand formation.

In greater detail, it can be inferred from the data of Scaria and Shafer (36) that under these conditions of ionic strength and pH, a temperature below 25°C is required for the ethidium cation exclusion process to dominate the net fluorescence signal. Given that intercalation occurs at a maximum of every 2.8 base triplets and once per 2.4 base pairs at 25°C, a 14% reduction in the amount of intercalated ethidium occurs upon triple-strand formation. However, within the triplex structure, the fluorescence quantum yield of the remaining intercalated ethidium cation increases by 19% for the $S_1 \rightarrow S_0$ electronic transition, thereby resulting in a net fluorescence intensity change of +2.3%. Therefore, direct correlation between the T_m for triplex formation and the onset of fluorescence emission with a positive temperature coefficient will be observed for systems of nucleic acids which have T_m values at or below ~25°C. This is consistent with our findings (Fig. 4) whereby the decrease in fluorescence intensity from the sensor correlates well with the temperature at which dT_{10} associates to the dT_{10}/dA_{10} duplex (T_m = 18°C). Although the transition for triple-strand formation between **1** and the immobilized dA_{10} occurs at 35°C (Fig. 6), a decrease in fluorescence intensity was not observed until the system was cooled to below ~25°C. In this regard, our fluorescence studies involving ethidium bromide binding to triple-helices is in full agreement with several earlier findings. Our system is then limited in terms of being able to identify the duplex to triplex transition temperature for nucleic acid systems with T_m values at or below 25°C. This does not, however, limit the applicability of this technology in terms of being a useful strategy to identify triplex formation.

It is also interesting to note in Figure 6, for the binding of **1** with immobilized dA_{10}, a significant fluorescence intensity is observed over the temperature range from ~50 to 60°C. This is indicative of the presence of intercalated ethidium cation. This is contrary to data presented in the UV denaturation/renaturation profiles for the same oligonucleotide system in solution where no significant quantity of complex formation exists over that temperature regime. A possible explanation for this unusual observation is that the ionic strength at or near the surface of the optical sensor may be greater than that of bulk solution owing to the presence of the immobilized polyanionic nucleic acid strands. As such, a shift in the T_m to higher temperatures would be expected. This is consistent with our previously reported data where binding of dA_{20} to immobilized dT_{20} was found to have a T_m value greater than that of the same oligonucleotide system in solution (14).

PAGE mobility retardation assay

Gel-shift experiments confirmed the interaction of ethidium bromide with the complexes observed in these studies. The electrophoretic mobility of the dT_{10}:dA_{10} duplex, both the Hoogsteen and reverse-Hoogsteen paired T·AT triplexes, and that of their component strands, was studied at 4°C. Following electrophoresis, the gels were visualized by UV shadowing, and by staining with ethidium bromide (Figs 7 and 8, respectively). The Hoogsteen triplex migrated more slowly than the duplex while the reversed-Hoogsteen triplex showed the slowest mobility of all, which is characteristic of branched nucleic acid structures (55). Association of **1** and dA_{10} was quantitative as evidenced by the complete disappearance of compound **1** and dA_{10}, when mixed in equimolar amounts, as visualized in the gel (Fig. 7). The stoichiometry of interaction between dT_{10} and dA_{10} for the duplex and Hoogsteen triplex was also confirmed by studies at different concentrations of the two oligonucleotides. When stained with ethidium bromide and illuminated by a UV lamp, fluorescence was observed only in the bands corresponding to the complexes, not single strands (Fig. 8). This is consistent with the well-known intercalative binding motif of ethidium bromide (56). As previously suggested by the biosensor studies, the **1**/dA_{10} reverse-Hoogsteen triplex gave the lowest fluorescence intensity, which could be caused by the limited availability of ethidium binding sites in this complex.

Conclusions

In conclusion, a novel method for the detection of triple-helical nucleic acid formation has been demonstrated. The complementary oligonucleotide, dT_{10}, which was expected to hybridize via a double-stranded Watson–Crick motif to immobilized dA_{10} provided a fluorescence intensity with a negative temperature coefficient upon cooling the system below the duplex melting temperature (T_m = 32°C). Upon further cooling, to the point where Hoogsteen T*AT triple-helix formation occurred, a fluorescence intensity change with a positive temperature coefficient was observed as a result of exclusion of the ligand from the triplex structure. Similar results were observed for triplex formation between dT_{10} and the immobilized dA_{10} sequence in both the normal (fiber-3′→5′) orientation and the reversed (fiber-5′→3′) orientation. The reversed-Hoogsteen T·AT triplex formed with **1** and the immobilized dA_{10} grown in reversed orientation (fibre-5′→3′) also provided a fluorescence intensity with a positive temperature coefficient, consistent with triplex formation and ligand exclusion. Correlation between the triplex T_m and the temperature at which the temperature coefficient of the fluorescence intensity changes from negative to positive may be observed for nucleic acid systems with a triplex T_m below ~25°C. Determination of triplex formation may be done rapidly (in minutes) by setting the initial temperature of the system to that of the triplex T_m and then slowly cooling the system (–0.5°C/min) for a few minutes to determine the fluorescence intensity temperature coefficient.

Further studies will be directed to expanding the triple-helix sequence context, investigations of mismatch sensitivity, and developing less limiting fluorescent dyes. Optical sensors with covalently bound intercalant have been created in our laboratories which provide a reagentless sensing system with fast response times (<6 min for full analytical response) for double-strand formation. Investigations of triplex formation on these reagentless sensors will also be evaluated in diagnostic assays, as they eliminate the problem of doubled-stranded DNA in the sample solution (e.g., in a biological sample) procuring all of the intercalant present in the buffer solution.

ACKNOWLEDGEMENTS

We acknowledge the Natural Science and Engineering Council of Canada (NSERC), and Le Fonds pour la Formation des Chercheurs et l'Aide à la Recherche (FCAR) for support of this work. We also acknowledge additional support from NSERC for a postgraduate scholarship awarded to P.A.E.P. and a postdoctoral scholarship awarded to R.H.E.H. We would also like to acknowledge Sebastien Robidoux for supplying the thermal renaturation data presented herein.

REFERENCES

1 Thomas, D. (1995) *BioTechnology*, **13**, 474–481.
2 Laval, J.M., Chopineau, J. and Thomas, D. (1995) *Trends Biotechnol.*, **13**, 474–481.
3 Hudson, R.H.E. and Damha, M.J. (1993) *J. Am. Chem. Soc*., **115**, 2119–2124.
4 Horn, T. and Urdea, M.S. (1989) *Nucleic Acids Res.*, **17**, 6959–6967.
5 Kool, E.T. (1996) *Annu. Rev. Biophys. Biomolec. Struct*., **25**, 1–28.
6 Chen, G. and Seeman, N.C. (1991) *Nature*, **350**, 631–633.
7 Ray, R.A., Cooper, P.J. and Wakefield, A.J. (1995) *BioTechnology*, **13**, 445–447.
8 McGown, L.B., Joseph, M.J., Pitner, J.B., Vonk, G.P. and Linn, C.P. (1995) *Anal. Chem*., **67**, A663–A668.
9 Millan, K.M., Saraullo, A. and Mikkelsen, S.R. (1994) *Anal. Chem.*, **66**, 2943–2948.
10 Su, H.B., Chong, S. and Thompson, M. (1996) *Langmuir*, **12**, 2247–2255.
11 Nilsson, P., Persson, B., Uhlén, M. and Nygren, P. (1995) *Anal. Biochem.*, **22**, 400–408.
12 Bates, P.J., Dosanjih, H.S., Kumar, S. Jenkins, T.C., Laughton, C.A. and Neidle, S. (1995) *Nucleic Acids Res*., **23**, 3627–3632.
13 Mirkin, C.A., Letsinger, R.L., Mucic, R.C. and Storhoff, J. (1996) *Nature*, **382**, 607–609.
14 Piunno, P.A.E., Krull, U.J., Hudson, R.H.E., Damha, M.J. and Cohen, H. (1995) *Anal. Chem.*, **67**, 2635–2643.
15 Graham, C.R., Leslie, D. and Squirrell, D.J. (1992) *Biosens. Bioelectron.*, **7,** 487–493.
16 Abel, A.P., Weller, M.G., Duveneck, G.L., Ehrat, M. and Widmer, H.M. (1996) *Anal. Chem.*, **68**, 2905–2912.
17 Strobel, S.A., Doucettestamm, L.A., Riba, L., Housman, D.E. and Dervan, P.B. (1991) *Science*, **254**, 1639–1642.
18 Maher, L.J., Dervan, P.B. and Wold, B. (1992) *Biochemistry*, **31,** 70–81.
19 Duvalvalentin, G., Thoung, N.T. and Hélène, C. (1992) *Proc. Nat. Acad. Sci. USA*, **89**, 504–508.
20 Stull, R.A. and Szoka, F.C.,Jr (1995) *Pharmceut. Res.*, **12**, 465–483.
21 Ito, T., Smith, C.L. and Cantor, C.R. (1992) *Proc. Natl. Acad. Sci. USA*, **89**, 495–498.
22 Wang, S.H., Friedman, A.E., Kool, E.T. (1995) *Biochemistry* **34**, 9774–9784.
23 Hoogsteen, K. (1959) *Acta Crystallogr*., **12**, 822–823.
24 Felsenfeld, G. Davies, D.R. and Rich, A. (1957) *J. Am. Chem. Soc*., **79**, 2023–2024.
25 Moser, H.E. and Dervan, P.B. (1987) *Science*, **238**, 645–650.
26 Praseuth, D., Perrouault, L., Doan, T.L., Chassignol, M., Thuong, N. and Hélène, C. (1988) *Proc. Natl. Acad. Sci. USA*, **85**, 1349–1353.
27 Cooney, M., Czernuszewicz, G., Postel, E.H., Flint, S.J. and Hogan, M.E. (1988) *Science*, **241**, 456–459.
28 Beal, P.A. and Dervan, P.B. (1991) *Science*, **251**, 1360–1363.
29 Miller, J.H. and Sobell, H.M. (1966) *Proc. Natl. Acad. Sci. USA*, **55**, 1201–1205.
30 Morgan, A.R. and Wells, R.D. (1968) *J. Mol. Biol*., **37**, 63–80.
31 Lee, J.S., Johnson, D.A. and Moran, A.R. (1979) *Nucleic Acids Res*., **6**, 3073–3091.
32 Hoogsteen, K. (1963) *Acta Crystallogr.* **16**, 907–916.
33 Waring, M.J. (1966) *Biochem. J*., **143**, 483–486.
34 LePecq, J.B. and Paoletti, C. (1967) *J. Mol. Biol*., **27**, 87–106.
35 Mergny, J.L., Collier, D., Rougée, M., Montenay-Garestier, T. and Hélène, C. (1991) *Nucleic Acids Res*., **19**, 1521–1526.
36 Scaria, P.V. and Shafer, R.H. (1991) *J. Biol. Chem.*, **266**, 5417–5423.
37 Maskos, U. and Southern, E.M. (1992) *Nucleic Acids Res*., **20**, 1679–1684.
38 Pon, R.T. (1993) In Agrawal, S. (ed.) *Methods in Molecular Biology—Protocols for Oligonucleotides and Analogs.* Humana Press, Totowa, NJ, Vol 20, 465–496.
39 Van de Sande, J.H., Ramsing, N.B., Germann, M.W., Elhorst, W., Kalisch, B.W., Kitzing, E.V., Pon, R.T., Clegg, R.C. and Jovin, T.M. (1988) *Science* **241**, 551–557.
40 Damha, M.J., Ganeshan, K., Hudson, R.H.E. and Zabarylo, S.V. (1992) *Nucleic Acids Res*., **20**, 6565–6573.
41 Damha, M.J. and Ogilvie, K.K., (1993) Agrawal, S. (ed.) *Methods in Molecular Biology—Protocols for Oligonucleotides and Analogs.* Humana Press, Totowa, NJ, Vol 20, pp 81–114.
42 Kibler-Herzog, L., Zon, G., Whittierm, G., Shaikh, M. and Wilson, W.D. (1993) *Anti-Cancer Drug Des*., **8**, 65–79.
43 Brennan, J.D., Brown, R.S., McClintock, C.P. and Krull, U.J. (1991) *Anal. Chim. Acta*, **237**, 253–263.
44 Hudson, R.H.E., Uddin, A. and Damha, M.J. (1995) *J. Am. Chem. Soc*., **117**, 12470–12477.
45 Salunkhe, M., Wu, T. and Letsinger, R.L. (1992) *J. Am. Chem. Soc.*, **114**, 8768–8772.
46 Fang, Y., Bai, C.L., Zhang, P.C., Cao, E.H. and Tang, Y.Q. (1994) *Science In China (Ser. B)*, **37**, 1306–1312.
47 Wolf, S.F., Haines, L., Fisch, J., Kremsky, J.N., Dougherty, J.P. and Jacobs, K. (1987) *Nucleic Acids Res.*, **15**, 2911–2926.
48 Hopkins, H.P., Hamilton, D.D.Wilson, W.D. and Zon, G. (1993) *J. Phys. Chem.*, **24**, 6555–6563.
49 Radhakrishnan, I., Patel, D.J., Priestly, E.S., Nash, H.M. and Dervan P.B. (1993) *Biochemistry*, **32**, 11228–11234.
50 Pilch, D., Levenson, C., Shafer, R. (1990) *Proc. Natl. Acad. Sci. USA*, **87**, 1942–1946.
51 Pilch, D.S., Brousseau, R. and Shafer, R.H. (1990) *Nucleic Acids Res.*, **18**, 5743–5750.
52 Fox, K.R. (1994) *Nucleic Acids Res.*, **22**, 2016–2021.
53 Cassidy, S.A., Strekowski, L., Wilson, W.D., and Fox, K.R. (1994) *Biochemistry*, **33**, 15338–15347.
54 Dagneaux, C., Liquier, J. and Taillandier, E. (1995) *Biochemistry*, **34**, 14815–14818.
55 Wallace, J.C. and Edmons, M. (1983) *Proc. Natl. Acad. Sci. USA*, **80**, 950–954.
56 Lim, C.S. (1994) *BioTechniques*, **17**, 626–628.